

Phases of the Infinite U Hubbard Model on Square Lattices

Li Liu,¹ Hong Yao,^{2,3} Erez Berg,⁴ Steven R. White,⁵ and Steven A. Kivelson¹

¹*Department of Physics, Stanford University, Stanford, California 94305, USA*

²*Department of Physics, University of California, Berkeley, California 94720, USA*

³*Materials Sciences Division, Lawrence Berkeley National Laboratory, Berkeley, California 94720, USA*

⁴*Department of Physics, Harvard University, Cambridge, Massachusetts 02138, USA*

⁵*Department of Physics, University of California, Irvine, California 92697, USA*

(Received 16 March 2011; published 22 March 2012)

We apply the density matrix renormalization group to study the phase diagram of the infinite U Hubbard model on 2- to 6-leg ladders. Where the results are largely insensitive to the ladder width, we consider the results representative of the 2D square lattice. We find a fully polarized ferromagnetic Fermi liquid phase when n , the density of electrons per site, is in the range $1 > n \geq 0.800$. For $n = 3/4$ we find an unexpected insulating checkerboard phase with coexisting bond-density order with 4 sites per unit cell and block-spin antiferromagnetic order with 8 sites per unit cell. For $3/4 > n$, all ladders with width > 2 have unpolarized ground states.

DOI: 10.1103/PhysRevLett.108.126406

PACS numbers: 71.10.Fd

The Hubbard model is the paradigmatic representation of strongly correlated electron systems [1]. It was introduced to explain ferromagnetism in transition metals [2,3], and, since then, has been studied as a model of antiferromagnetism, unconventional superconductivity, cold atoms in optical lattices, and exotic fractionalized phases of quantum matter. In the $U \rightarrow \infty$ limit (in units in which the hopping $t = 1$) there are no parameters other than n , the electron density per site. Despite the apparent simplicity of this limit, relatively little is known about its phase diagram. Nagaoka's theorem [4] states that for a finite size system with one doped hole away from half filling ($n = 1$), the ground state is fully spin polarized. However, it has been controversial whether this state survives a finite range of hole concentrations in the thermodynamic limit. Previous exact diagonalization [5], Monte Carlo [6], and variational [7–9] studies suggest that the fully polarized or “half metallic ferromagnetic” (HMF) state persists over a finite range of densities, $1 > n > n_F$ with $n_F < 1$. In contrast, other lines of analysis [10–13] were suggestive that $n_F \rightarrow 1^-$.

In this Letter we report the results of an extensive density matrix renormalization group (DMRG) study of the zero temperature ($T = 0$) phase diagram of the Hubbard model in the $U \rightarrow \infty$ limit, as a function of n , the density of electrons per site. To begin with, we study the 2-leg ladder on systems of size up to 2×50 (typical truncation error 10^{-8} – 10^{-13}), large enough that finite size scaling can be used to obtain clear convergence to the thermodynamic limit. The resulting phase diagram is shown in the lower panel of Fig. 1. To get a feeling for which features of the 2-leg Hubbard ladder extrapolate smoothly to 2D, we compute the properties of 4-leg and 6-leg ladders (with sizes up to 4×20 and 6×16 , with corresponding truncation errors $\sim 10^{-6}$ and 10^{-4} , respectively). The inferred partial phase diagrams of these wider

ladders are shown in the two middle panels of Fig. 1. (We have also carried out limited additional studies of 3- and 5-leg ladders.) While there may be subtle correlations characteristic of the 2D model that would only be manifest were we able to study wider or longer ladders, many features of the phase diagram are already remarkably insensitive to ladder width and length for the studied system sizes. We therefore speculate that these features survive as ground-state phases of the fully 2D model, as shown in the upper panel of Fig. 1.

We summarize our main findings. (1) For $1 > n > n_F$, we find a HMF phase, i.e., a fully spin-polarized Fermi liquid. For all even leg ladders we have studied $n_F = 0.800$, so we expect that in 2D, $n_F \approx 0.800$ as well, in agreement with recent variational studies [8].

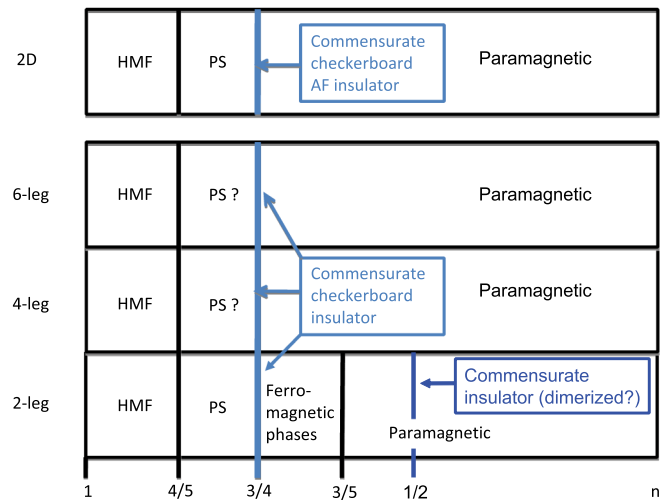


FIG. 1 (color online). The phase diagrams of the infinite U Hubbard model on the 2-, 4-, and 6-leg ladders, and the inferred phase diagram in 2D.

(2) For $n_F > n > 3/4$, the 2-leg ladder appears to phase separate (PS), with the two coexisting phases having densities $n = n_F$ and $n = 3/4$. Our more limited results on broader ladders suggest that the same holds true for 4-leg ladders and, by extension, in 2D as well [14]. (3) For $n = 3/4$, the 2-leg ladder forms an insulating commensurate plaquette density wave state, as shown schematically in Fig. 2(a). This pattern of symmetry breaking suggests that the spin degrees of freedom on “strong” $3/2$ -spin plaquettes are coupled antiferromagnetically through “weak” bonds; indeed there is no detectable spin gap and we find clear signatures of quasi-long-range antiferromagnetic order with twice the period of the plaquette order. The 4-leg and 6-leg ladders exhibit a similar (slightly weaker) ordering tendency, forming the checkerboard plaquette order of the sort shown in Figs. 2(b) and 2(c); given the results on 2-, 4-, and 6-leg ladders we suggest that the corresponding phase persists in the 2D limit. The 2D checkerboard phase has coexisting bond-density wave and block-spin antiferromagnetic order. However, the site-charge density in this phase is uniform. The existence of this phase, and its apparent robustness, was unanticipated in previous studies as far as we know. (4) For $n < 3/4$, the ground state of the 2-leg ladder exhibits ferromagnetic or paramagnetic phases depending on n . However, the ground state is always paramagnetic for the 4- and 6-leg ladders, which indicates a paramagnetic ground state in 2D.

DMRG applied to Hubbard ladders.—The Hubbard model is defined, as usual, by

$$H = -t \sum_{\langle ij \rangle, \sigma=\uparrow, \downarrow} [c_{i\sigma}^\dagger c_{j\sigma} + \text{H.c.}] + U \sum_i c_{i\uparrow}^\dagger c_{i\downarrow}^\dagger c_{i\downarrow} c_{i\uparrow}, \quad (1)$$

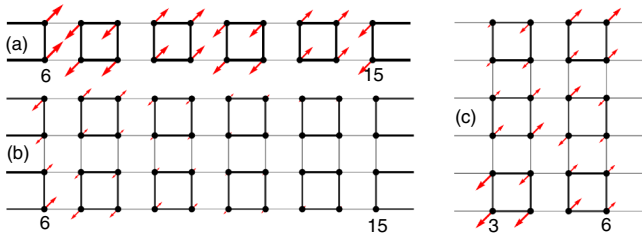


FIG. 2 (color online). Ground-state correlations at $n = 3/4$ for a central portion of (a) the 2×20 ladder, (b) the 4×20 ladder, (c) the 6×8 ladder. The thickness of the lines is proportional to the third power of the magnitude of B_{ij} , and the length of the arrows to the magnitude of S_j , where the axis of spin quantization is set by a Zeeman field of strength $h = 1$ applied to the lower left-hand site of each ladder. The numbers index the position along the ladder. For the 2×20 ladder, the values of B_{ij} in the figure range from $B_{ij} = 0.30$ (lightest line) to $B_{ij} = 0.45$ (darkest line), while the magnitude of S_j ranges from -0.19 to 0.21 . For the 4×20 ladder B_{ij} ranges from 0.30 to 0.41 , while S_j ranges from -0.12 to 0.12 . For the 6×8 ladder B_{ij} ranges from $B_{ij} = 0.31$ to 0.41 , while S_j ranges from -0.18 to 0.16 . (We have obtained similar results for a 6×16 ladder, but even keeping 18 000 states, the convergence is not as complete as for the smaller ladders.)

where $c_{j\sigma}^\dagger$ creates an electron with spin polarization σ on site j and $\langle ij \rangle$ signifies pairs of nearest-neighbor sites. In the limit $U \rightarrow \infty$, the Hamiltonian is parameter free; the second term in H is replaced by the nonholonomic constraint of no double occupancy, $\sum_{\sigma} c_{j\sigma}^\dagger c_{j\sigma} = 0$, or 1 , and we take units of energy so that $t = 1$.

The DMRG calculations were carried out keeping 4000–18 000 states. All ladders were taken to have open boundary conditions in both directions. When we compute the expectation value of various densities, it is sometimes useful to break spin rotational symmetry by applying a Zeeman field of magnitude $h = 1$ in the z direction on the single site at the lower left-hand end of the ladder.

To characterize the excitation spectrum of the system, we define the charge, spin, and single-particle gaps, Δ_c , Δ_s , and Δ_{1p} , as follows:

$$\begin{aligned} \Delta_c &\equiv [E(N_{\text{el}} + 2) + E(N_{\text{el}} - 2) - 2E(N_{\text{el}})]/2 \\ \Delta_s &\equiv [E(S = 1; N_{\text{el}}) - E(S = 0; N_{\text{el}})], \end{aligned} \quad (2)$$

$$\Delta_{1p} \equiv [E(N_{\text{el}} + 1) + E(N_{\text{el}} - 1) - 2E(N_{\text{el}})],$$

where N_{el} is the total number of electrons (which is often taken, for present purposes, to be even), and $E(N_{\text{el}})$ and $E(S, N_{\text{el}})$ are, respectively, the ground-state energy and the ground-state energy in a given spin sector. This definition of the spin gap is only useful under circumstances in which the ground state has $S = 0$. Where possible, we have extrapolated values of the gaps to the thermodynamic limit by fitting the data from finite length ladders to a quadratic form, $\Delta(N) = \Delta + AN^{-1} + BN^{-2}$, where N is the length of the ladders.

Results for the 2-leg ladder.—We have computed the ground-state properties of the 2-leg ladder as a function of n for system sizes $2 \times N$ with $N = 20, 30, 40$, and 50 . To identify the ferromagnetic portions of the phase diagram, we have computed the ground-state magnetization density $M = S/S_{\text{max}}$, where S is the total spin of the ground state, and $S_{\text{max}} = Nn$ is the maximum possible value of S in a fully spin-polarized state. The results are shown in Fig. 3(a), where different curves denote the different system sizes (see Supplemental Material [16] for part of the raw data including error bar). Since the four curves are nearly identical, the extrapolation to the thermodynamic limit is trivial. Specifically, (1) The fully polarized ground state terminates at $n = n_F = 4/5$, independent of N [17] (see Supplemental Material [16] for supporting raw data). This value of n_F is not locked by any obvious commensurability effect that we have detected. For instance, if we modify the Hamiltonian by making the hopping matrix elements on the rungs $t' = 0.5t$, where t is the hopping matrix element on the legs of the ladder, we find that $n_F = 0.85$. However $n_F = 4/5$ is robust when t' is increased, at least up to $t' = 2t$. (2) The ground state at $n = 3/4$ is an insulating paramagnetic state with a charge gap, $\Delta_c = 0.24 \pm 0.02t$, a single-particle gap, $\Delta_{1p} = 0.245 \pm 0.02t$, but a vanishing spin gap $\Delta_s < 3 \times 10^{-4}t$ which is zero

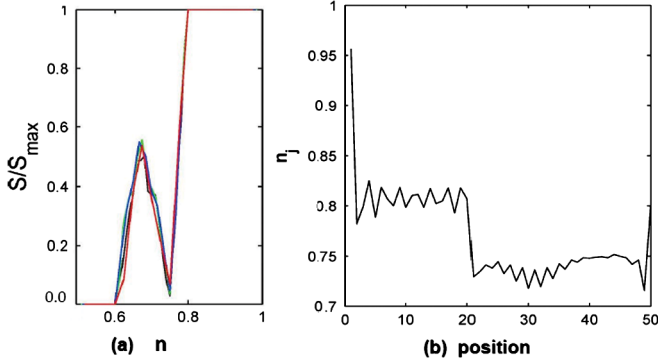


FIG. 3 (color online). (a) Magnetization, normalized to its maximum possible value, of the 2-leg ladder as a function of n . The four highly overlapping curves correspond, respectively, to $N = 50, 40, 30$, and 20 . (b) Expectation value of the site density, n_j , in a 2×50 ladder with average density $n = 0.77$ and a chemical potential of magnitude $\mu = 0.3t$ applied to the leftmost 2×20 sites.

within our uncertainty. (See Supplemental Material [16] for raw data used for extrapolation.) The character of this state on a central segment of the ladder is shown in Fig. 2(a). The thickness of the lines on the bonds between sites represents the magnitude of the expectation value of the bond density, $B_{ij} \equiv \sum_{\sigma} \langle [c_{i\sigma}^{\dagger} c_{j\sigma} + \text{H.c.}] \rangle$ and the length of the arrow on the site represents the expectation value of the spin on that site, $S_j \equiv \frac{1}{2} \sum_{\sigma} \sigma \langle c_{j\sigma}^{\dagger} c_{j\sigma} \rangle$. A Zeeman field of strength 1 has been applied to the first site on the lower leg of the ladder; translation symmetry is broken as well by the ends of the ladder. There is a period-2 bond-density wave, with a magnitude that does not decrease with distance from the end of the ladder, nor does it depend significantly on the length of the ladder; this signifies a discrete, broken translation symmetry. There is also a period-4 ordering tendency of the spin density, but with an intensity which decays slowly with distance from the end at which the Zeeman field is applied. This, and the absence of a spin gap, signifies that there is quasi-long-range antiferromagnetic order. The expectation value of the electron density, $n_j \equiv \sum_{\sigma} \langle c_{j\sigma}^{\dagger} c_{j\sigma} \rangle$, is nearly uniform, $n_j \approx n$ for all j except in the immediate vicinity of the ends of the ladder. To summarize, at $n = 3/4$ the system forms a “plaquette density wave,” which can be visualized as a checkerboard array of weakly coupled plaquettes, each with three electrons in a state of total spin $3/2$, and a weak, antiferromagnetic exchange coupling between plaquettes. As one would expect, the character of this state is not sensitive to small changes in the Hamiltonian—for instance, if we set the rung hopping $t' = 0.5t$ or $2t$, we find no qualitative change in the insulating phase at $n = 3/4$. (3) When n is in the range $4/5 > n > 3/4$ the ground state appears to be a 2-phase mixture of the fully polarized state with $n = 4/5$ and the checkerboard state with $n = 3/4$. The evidence for this is as follows: (a) as seen in Fig. 3(a), the ground-state magnetization is (within expected finite

size corrections) a linear function of n in this range. (b) The ground-state energy (not shown) is, to similar accuracy, a linear function of n in this range, with a continuous first derivative at $n = n_F$; this is precisely the behavior expected from a Maxwell construction for a two-phase region. (c) As a final test, we have applied an on-site potential of magnitude $\mu = 0.3t$ to the leftmost 2×20 lattice sites of a 2×50 ladder with mean value of $n = 0.77$; as can be seen in Fig. 3(b), the resulting density profile consists of a region with density $n_j \approx 4/5$ on the left portion, and $n_j \approx 3/4$ on the right portion of the ladder, with a sharp domain wall separating them. We have also computed spin correlation function for direct evidence. However, the expected two peaks are broadened due to numerical uncertainty (see Supplemental Material [16] for results). (4) Again from Fig. 3(a), it is apparent that for $3/4 > n > 3/5$, there is a regime in which the ground state is partially spin polarized, with maximal spin polarization being attained at $n = 2/3$, where $M \approx 0.5$. The behavior of the 2-leg ladder in this regime is interesting in its own right, but, in contrast to the situation in other ranges of n , similar behavior is not seen in wider ladders. (5) For $3/5 > n$, the ground state has $M = 0$. Finite size scaling leads to the speculation that, for $n \neq 1/2$, this is a Luttinger liquid (LL) phase with Δ_c , Δ_s , and Δ_{1p} all tending to 0 in the thermodynamic limit to within our numerical uncertainty of $\sim 0.02t$. (Clearly, in a Fermi liquid (FL), all three gaps vanish in the thermodynamic limit. In 1D, the FL is unstable in the presence of any interactions, but there exists a stable gapless LL.) (6) For $n = 1/2$ there is a clearly identifiable charge gap, $\Delta_c \sim 0.1t$. One can think of this as arising from a state in which there is a single electron localized on each rung of the ladder [18] so that the spin-degrees of freedom form an effective spin-1/2 chain, and thus can be expected to exhibit one of two possible phases—a gapless phase with power law antiferromagnetic and dimerization correlations or a long-range ordered dimerized phase with a spin gap. In a forthcoming paper we find slowly decaying dimerization and antiferromagnetic correlations, which are suggestive of the undimerized phase.

Results for wider ladders and extension to 2D.—Wider ladders provide necessary clues concerning the evolution of the phase diagram as the 2D limit is approached. However, with increasing width, it becomes more difficult to obtain fully converged results from DMRG; thus, we use increasingly shorter ladders as the width increases.

To study the evolution of the HMF phase, we have computed n_F , the largest value of n for which the ground state is fully spin polarized, for a variety of ladders (see Supplemental Material [16] for results). An even-odd effect is apparent. For the $3 \times N$ ladders $n_F = 0.87$, independent of N , while for $4 \times N$ (as for $2 \times N$) $n_F = 0.8$. For 5- and 6-leg ladders, we were restricted to relatively small N , but the trend continues, with n_F slightly greater than 0.8 for the 5 leg and approximately equal to 0.8 for the 6 leg.

Extrapolating either the even or the odd leg ladder results to the 2D limit results in an estimate of $n_F \approx 0.8$ as the ladder width tends to infinity.

We exhibit in Figs. 2(b) and 2(c), respectively, the ground-state correlations at $n = 3/4$ of the longest accessible 4- and 6-leg ladders. The analogous commensurate checkerboard state we found in the 2-leg ladder is manifest in these correlations, as well. Indeed, the magnitude of the broken symmetry does not seem to decrease much with increasing ladder width—see figure caption.

For the 4×20 ladder with $n = 3/4$, $\Delta_c = 0.23 \pm 0.006t$ and $\Delta_s = 0.008 \pm 0.002t$. For comparison, on the 2×20 ladder, the charge gap is of comparable magnitude, $\Delta_c = 0.286 \pm 0.006t$, but the spin gap is more than a factor of 20 smaller, $\Delta_s < 0.0003t$. The robustness of the charge gap corroborates the existence of a commensurate insulating checkerboard state. To the extent that we can think of the low energy spin degrees of freedom as corresponding to a spin $3/2$ antiferromagnet defined on the checkerboard lattice, all $(4p + 2)$ -leg and $4p$ -leg ladders correspond, respectively, to $(2p + 1)$ -leg and $2p$ -leg spin $3/2$ Heisenberg ladders, and accordingly are expected to be gapless, or to exhibit a spin gap, albeit one which falls exponentially with increasing n [19]. Together, these observations strongly support the conclusion that the checkerboard antiferromagnet is the ground-state phase in the 2D limit.

For $n_F > n > 3/4$, we have not yet carried out serious calculations to test for phase separation. However, the apparent existence of partial polarization and the robustness of the plaquette phase at $n_F = 3/4$ suggests that, as for the 2-leg ladder, phase separation is likely for the 4- and 6-leg ladders, and by extension, in the 2D limit.

Finally, we have found that the ground states of all the 4-leg ladders we have investigated have total spin ≤ 2 for $3/4 > n > 3/5$ and total spin ≤ 1 for $3/5 > n$, respectively, corresponding to $M \approx 0$. In the near future we also hope to study the apparent LL phase to determine whether there is a well-defined strong coupling limit [20] of the superconducting state that is known to arise at weak coupling [21].

Conclusion.—Our extensive DMRG study of the $U \rightarrow \infty$ limit Hubbard model on the 2-, 4-, and 6-leg ladders strongly indicates that in the 2D thermodynamic limit the ground state is a fully spin polarized Fermi liquid for a finite range $1 < n < n_F$ with $n_F \approx 0.8$. Also unexpectedly, entrance into the paramagnetic phase for $n > 3/4$ is marked by a commensurate checkerboard phase at $n = 3/4$ of substantial robustness. While we have not yet investigated the effects of nonzero t/U , we expect the HMF to be stable so long as $1 - \alpha\sqrt{t/U} > n > n_F$, where α is a number of order 1 [22].

We sincerely thank D.-H. Lee, F. Yang, G. Karakonstantakis, H. Zhang, B. Yan, and B. Moritz for helpful discussions. This work was supported by DOE

Grant No. DE-AC02-76SF00515 at Stanford (L. L. and S. A. K.), DOE Grant No. DE-AC02-05CH11231 at Berkeley (H. Y.), NSF Grants No. DMR-0757145 (E. B.), No. DMR-0705472 (E. B.), and No. DMR-0907500 (S. R. W.).

-
- [1] For a recent review, see D. J. Scalapino, in *Handbook of High-Temperature Superconductivity*, edited by J. Schrieffer and J. Brooks (Springer, New York, 2007), pp. 495–526.
 - [2] M. C. Gutzwiller, *Phys. Rev. Lett.* **10**, 159 (1963).
 - [3] J. Hubbard, *Proc. R. Soc. A* **276**, 238 (1963).
 - [4] Y. Nagaoka, *Phys. Rev.* **147**, 392 (1966).
 - [5] See, for example, J. A. Riera and A. P. Young, *Phys. Rev. B* **40**, 5285 (1989).
 - [6] M. Brunner and A. Muramatsu, *Phys. Rev. B* **58**, R10100 (1998).
 - [7] F. Becca and S. Sorella, *Phys. Rev. Lett.* **86**, 3396 (2001).
 - [8] G. Carleo, S. Moroni, F. Becca, and S. Baroni, *Phys. Rev. B* **83**, 060411(R) (2011).
 - [9] See, for example, C.-C. Chang, S. Zhang, and D. M. Ceperley, *Phys. Rev. A* **82**, 061603(R) (2010); S.-Y. Chang, M. Randeria, and N. Trivedi, *Proc. Natl. Acad. Sci. U.S.A.* **108**, 51 (2010).
 - [10] See, for example, G.-S. Tian, *Phys. Rev. B* **44**, 4444 (1991), and references therein.
 - [11] M. Takahashi, *J. Phys. Soc. Jpn.* **51**, 3475 (1982).
 - [12] B. Douçot and X. G. Wen, *Phys. Rev. B* **40**, 2719 (1989).
 - [13] W. O. Putikka, M. U. Luchini, and M. Ogata, *Phys. Rev. Lett.* **69**, 2288 (1992).
 - [14] A. Tandon, Z. Wang, and G. Kotliar, *Phys. Rev. Lett.* **83**, 2046 (1999).
 - [15] This phase was found previously for $U/t > 18.6$ in the checkerboard Hubbard model with weak coupling between plaquettes, i.e., with explicit translation symmetry breaking—see H. Yao, W.-F. Tsai, and S. A. Kivelson, *Phys. Rev. B* **76**, 161104(R) (2007); its existence may have been implicit in the small size exact diagonalization study of Z. Song and H. Shen, *Phys. Rev. B* **47**, 14576 (1993).
 - [16] See Supplemental Material at <http://link.aps.org/supplemental/10.1103/PhysRevLett.108.126406> for an illustration of the application of edge magnetic field, lists of raw data, and a plot of the Fourier transform of spin correlation function in the phase separation region.
 - [17] Similar results on shorter ladders were obtained previously by S. Liang and H. Pang, *Europhys. Lett.* **32**, 173 (1995).
 - [18] M. Kohno, *Phys. Rev. B* **56**, 15015 (1997) studied the charge gap in the 2-leg ladder with $n = 1/2$ as a function of t'/t , where for large t'/t the intuitive picture becomes exact.
 - [19] S. Chakravarty, *Phys. Rev. Lett.* **77**, 4446 (1996).
 - [20] P. A. Casey and P. W. Anderson, *Phys. Rev. Lett.* **106**, 097002 (2011).
 - [21] S. Raghu, S. A. Kivelson, and D. J. Scalapino, *Phys. Rev. B* **81**, 224505 (2010).
 - [22] E. Eisenberg *et al.*, *Phys. Rev. B* **65**, 134437 (2002).